International Journal of Computational Intelligence Systems
Vol. **13(1)**, 2020, *pp.* 1608–1618
DOI: https://doi.org/10.2991/ijcis.d.201012.005; ISSN: 1875-6891; eISSN: 1875-6883
https://www.atlantis-press.com/journals/ijcis/

Research Article

An Evolutionary Self-organizing Cost-Sensitive Radial Basis Function Neural Network to Deal with Imbalanced Data in Medical Diagnosis

Jia-Chao Wu[1], Jiang Shen[1], Man Xu[2,*], Fu-Sheng Liu[1]

[1]*College of Management and Economics, Tianjin University, Tianjin, 300072, China*
[2]*Business School, Nankai University, Tianjin, 300071, China*

ARTICLE INFO

Article History
Received 27 Jul 2020
Accepted 28 Sep 2020

Keywords
Imbalanced data
Medical diagnosis
Radial basis function neural network
Cost-sensitive
Genetic algorithm
Particle swarm optimization

ABSTRACT

Class imbalance is a common issue in medical diagnosis. Although standard radial basis function neural network (RBF-NN) has achieved remarkably high performance on balanced data, its ability to classify imbalanced data is still limited. So far as we know, cost-sensitive learning is an advanced imbalanced data processing method. However, few studies have focused on the combination of RBF-NN and cost sensitivity. From our knowledge, only one paper has proposed a cost-sensitive RBF-NN for software defect prediction. However, the authors implemented a fixed RBF-NN structure. In this paper, a novel cost-sensitive RBF-NN that optimizes structure and parameters simultaneously is proposed to handle medical imbalanced data. Genetic algorithm (GA) and improved particle swarm optimization (IPSO) are used to optimize the structure and parameters of cost-sensitive RBF-NN respectively, and the optimization of cost-sensitive RBF-NN based on dynamic structure is realized. A cost-sensitive function determined adaptively by the sample distribution as the objective function of RBF-NN, so that it can adapt to datasets with different sample distributions. Experimental results show that the proposed cost-sensitive RBF-NN outperforms other state-of-the-art representative algorithms for five imbalanced medical diagnostic datasets in term of accuracy and area under curve (AUC). It can improve the accuracy of medical diagnosis and reduce the error rate of medical decisions.

1. INTRODUCTION

In the last decades, classification systems have played an important role in medical diagnosis [1]. It not only can help doctors reduce the diagnostic error rate, it also can increase efficiency. However, the number of patients with various pathologies in medical datasets is often different, which makes the distribution of the dataset imbalanced [2]. Dealing with datasets with imbalanced class distribution poses a challenge to classifiers [3,4].

Imbalanced data refers to the fact that one class in the dataset is significantly larger than the other classes [5]. The class with a small number of samples is called minority class, and the class with a large number of samples is called majority class. Traditional machine learning algorithms treats the misclassification costs of different classes equally, which results in classifiers tend to focus on majority class [6]. But in the case of imbalanced data, the cost for minority class misclassification is often higher than that for majority class. For example, the cost of misclassifying a patient as a normal person is much greater than the opposite decision, so dealing with imbalanced data is essential for medical diagnosis. Various methods have been developed so far to handle this problem. Shilaskar *et al.* [2] proposed a modified particle swarm optimization (MPSO) for pathological multiclass imbalanced datasets. Experimental results show that MPSO is better than the other five compared algorithms. A method combining information granularity and clustering is established to deal with imbalanced data [7]. This method effectively improves the performance of prostate cancer prognosis prediction. Very recently, Gan *et al.* [4] propose an integrated tree augmented naive bayes network (TANBN) with cost-sensitive classification method. This method is used to process medical imbalanced data, and obtains high accuracy and area under curve (AUC).

Among the many imbalanced learning methods, cost-sensitive learning is one of the most advanced methods. For different classes, the cost-sensitive classifier will set different misclassification values, and then train the classifier by minimizing the expected cost [8]. In recent years, many cost-sensitive methods have been proposed to deal with imbalanced data and have obtained satisfactory results, such as MetaCost [9], cost-sensitive artificial neural network (ANN) [10], cost-sensitive k-nearest neighbor (KNN) [11]. However, few researchers pay attention to the combination of radial basis function neural network (RBF-NN) and cost-sensitivity. RBF-NN is a special neural network with only one hidden layer. Due to its better approximation ability of complex nonlinear problems, convergence speed, and simple topology [12], RBF-NN has been widely adopted in various prediction problems [13–15]. From our

*Corresponding author. Email: td_xuman@nankai.edu.cn

knowledge, only literature [16] has proposed an adaptive dimensional biogeography optimized cost-sensitive RBF-NN for software defect prediction. However, the authors implemented a fixed RBF-NN structure, which is often not as good as the results obtained by optimizing the structure and parameters simultaneously [17]. In recent years, genetic algorithm (GA) and particle swarm optimization (PSO) as two popular evolutionary methods that have been successfully applied to the simultaneous optimization of RBF-NN structure and parameters. Li *et al.* [18] proposes a modified PSO based on multi-Gbest strategy to optimize the structure and parameters of RBF-NN simultaneously and applies this method to estimate aero-engine thrust. Jia *et al.* [19] propose to optimize the architecture and radial basis function parameters of RBF-NN with GA, and then apply the optimized RBF-NN combined with partial least squares to small sample classification. From the previous works, most researchers are concerned with the optimization of conventional RBF-NN. But conventional RBF-NN assumes that the cost of misclassification for each class is equal, which makes it not good at handling imbalanced data. In summary, it is necessary to propose a cost-sensitive RBF-NN with optimized structure and parameters simultaneously.

Based on the above considerations, in this paper, we propose an evolutionary self-organizing cost-sensitive RBF-NN co-optimized by GA and improved particle swarm optimization (IPSO) to handle medical imbalanced data. The IPSO algorithm proposed by Montazer and Giveki [20] adopts an adaptive dynamic adjustment strategy to improve the inertial weight and position update, which has better adaptability to highly nonlinear and complex problems. Specifically, we binary code the hidden layer units of the RBF-NN and use GA for evolution. For the center, radius, and weight of the RBF-NN, we use real-value encoding and optimized it by IPSO. This is because PSO has a deeper intelligent background and is easier to implement for real-value optimization problems [21]. Moreover, a cost-sensitive function determined by the sample distribution is used as the fitness function of GA and IPSO. This cost-sensitive function is also the objective function of RBF-NN. The main contributions of this study are as follows:

- A novel cost-sensitive RBF-NN that optimizes structure and parameters simultaneously is proposed to handle medical imbalanced data.
- GA and IPSO are used to optimize the structure and parameters of cost-sensitive RBF-NN respectively, and the optimization of cost-sensitive RBF-NN based on dynamic structure is realized.
- The algorithm uses a cost-sensitive function determined adaptively by the sample distribution as the objective function of RBF-NN, so that it can adapt to datasets with different sample distributions.
- The proposed method can improve the accuracy of medical diagnosis and reduce the error rate of medical decisions for five medical problems with imbalanced class distribution.

The remainder of this paper is structured as follows: we review previous research on imbalanced data processing methods in Section 2. The proposed method is shown in Section 3. Section 4 is concerned with experimental results and discussion. Lastly, conclusions are drawn in Section 5.

2. RELATED WORKS

The existing research on imbalanced data processing methods has two main research directions: data-based methods and algorithm-based methods [22]. We will review and analyze the advanced methods of imbalanced data processing in recent years from these two aspects.

The data-based processing methods balances the class distribution by resampling the original data. Resampling methods can be divided into three groups: undersampling, oversampling, and hybrid sampling. Undersampling method improves the sample distribution of the data by reducing the number of majority class samples, such as cluster-based [23,24] and evolution-based methods [25,26]. Although the undersampling methods can improve classification accuracy, it may cause loss of information [27]. In contrast to the undersampling methods, oversampling techniques handle the imbalanced data by repetition of present minority samples or creating new ones. Synthetic minority oversampling technique (SMOTE) is one of the most representative and widely used oversampling algorithms [28]. Its main idea is to generate new samples based on the difference of the feature vectors of minority class samples with their neighbors. Although SMOTE is a simple and effective oversampling method, its blind sampling may make the classification result worse [29,30]. To overcome this drawback, several oversampling methods have been proposed, such as Geometric SMOTE [31] and LR-SMOTE [32], to selectively replicate the minority class samples. In addition, there are some methods of mixing oversampling and undersampling, such as SMOTE-Tomek Link [33].

Algorithm-based processing of imbalanced data mainly involves two aspects: ensemble method and cost-sensitive method. For the aspect of ensemble learning, the ensemble classifier enhances the efficiency of a single classifier by integrating multiple classifiers [34]. Roughly, in approximately two groups can be divided into current ensemble learning methods: iterative and parallel [35]. Boosting is the most common and effectively iterative-based ensemble method. It trains multiple weak classifiers by adjusting the weight distribution of the training data, and combines them linearly to form a strong classifier, such as Adaboost [36], GBDT [37]. For parallel-based ensembles, it means that each base classifier can be trained in parallel, such as bagging, resampling- based ensembles [38–40]. As for cost-sensitive learning, cost-sensitive neural networks are one of the rapidly developing cost-sensitive methods in recent years. A cost-sensitive convolutional neural network has been proposed to identify abnormal industrial control chart patterns [41]. Li *et al.* [42] proposed a cost-sensitive deep neural network for sequential three-way decision-based image data analysis. A cost-sensitive ANN optimized by artificial bee colony algorithm is proposed to predict software defects [43]. This method optimizes weights and structure of the ANN is selected by trial and error.

Different from previous studies, we proposed an evolutionary self-organizing cost-sensitive RBF-NN jointly optimized by GA and IPSO. This method can optimize both the structure and parameters of RBF-NN simultaneously. The algorithm uses a cost-sensitive function determined adaptively by the sample distribution as the objective function of RBF-NN, so that it can adapt to datasets with different sample distributions.

3. METHODS

3.1. Radial Basis Function Neural Network

RBF-NN has better nonlinear approximation and convergence speed than back propagation networks. It has been proven that RBF-NN can approximate any continuous function if there are a sufficient number of radial basis function neurons [44]. Figure 1 shows the architecture of RBF-NN. Consider an n-dimensional input vector $\mathrm{X} = [x_1, x_2, ...x_n]^T$, the output of RBF-NN can be calculated as follows:

$$\mathrm{Y} = \sum_{i=1}^{m} \mathrm{w}_{ij}\phi_i(\boldsymbol{X}), i = 1, 2, ..., m \;\; j = 1, 2, ..., k \tag{1}$$

where m and k are the number of hidden units and output units, respectively. w_{ij} is the output weight between ith hidden unit and jth output unit. $\phi_i(\mathrm{X})$ is the radial basis function of ith hidden unit, which can be defined as follows:

$$\phi_i(\boldsymbol{X}) = exp\left(-\frac{\|\boldsymbol{X} - c_i\|^2}{2r_i^2}\right), \; i = 1, 2, ..., m \tag{2}$$

where c_i and r_i are the center and radius of ith radial basis function.

In general, training RBF-NN can be separated into two stages: first of all, determine the center and radius of radial basis function by an unsupervised method. Then, apply the supervised method to determine the output weight. Appropriate structure and parameters are very important for RBF-NN. For a better performance, it is necessary to consider the collaborative optimization of the structure and parameters of RBF-NN.

3.2. Genetic Algorithm

Holland proposed GA in the 1970s [45]. Typical GA evolve individuals based on fitness and selection, crossover, and mutation operators. In selection operator, chromosomes are chosen as parents from the population. The larger the fitness value, the greater the probability of being selected. In crossover operator, some genes are exchanged between chromosomes, creating new chromosomes. Then in mutation operator, one or more gene in the chromosome are randomly perturbed (often with a low probability).

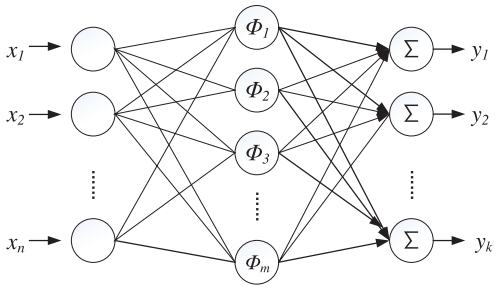

Figure 1 | The architecture of radial basis function neural network (RBF-NN).

3.3. Improved PSO (IPSO)

Particle swarm optimization (PSO) is a swarm intelligence optimization algorithm, which imitates the behavior of birds foraging. In the PSO algorithm, each particle is a feasible solution to the optimization problem. The movement of particles is affected by its previous optimal solution and global optimal solution. and its position is updated according to the speed. The velocity and position of each particle is updated as follows:

$$v_{id}^{t+1} = \omega v_{id}^{t} + \mathrm{l}_1\mathrm{R}_1\left(pb_{id}^{t} - x_{id}^{t}\right) + \mathrm{l}_2\mathrm{R}_2\left(gb_{d}^{t} - x_{id}^{t}\right) \tag{3}$$

$$x_{id}^{t+1} = x_{id}^{t} + v_{id}^{t+1} \tag{4}$$

where v_{id}^{t} is the velocity of particle i in the d-th dimension at the t-th iteration. l_1 and l_2 denote individual and social learning factors, respectively. R_1 and R_2 are random numbers between 0 and 1, pb_{id}^{t} and gb_{d}^{t} are the best previous position for particle i and all particles along the d-th dimension at the t-th iteration, respectively. ω is inertia weight.

For a better performance, we usually hope that particles have a powerful global search capability in the early stages of evolution and good local exploration capability in the late stage of evolution. IPSO adopts an adaptive dynamic adjustment strategy to improve the inertial weight and position update, which has better adaptability to highly nonlinear and complex problems. The dynamic adjustment strategy of the IPSO is as follows:

$$x_{id}^{t+1} = x_{id}^{t} + u_i^t v_{id}^{t+1} \tag{5}$$

$$u_i^t = \begin{cases} \left(\mathrm{v}_{\max}/v_i^t\right)\mathrm{e}^{-\left(t/\mathrm{t}_{\max}\right)^2} & \text{if } v_i^t > \mathrm{v}_{\max} \\ 1 & \text{if } \mathrm{v}_{\min} < v_i^t < \mathrm{v}_{\max} \\ \left(\mathrm{v}_{\min}/v_i^t\right)\mathrm{e}^{-\left(t/\mathrm{t}_{\max}\right)^2} & \text{if } v_i^t < \mathrm{v}_{\min} \end{cases} \tag{6}$$

$$\omega_i^t = \mathrm{k}_1 h_i^t + \mathrm{k}_2 b_i^t + \omega_0 \tag{7}$$

$$h_i^t = \left|\left(\max\left\{F_{id}^t, F_{id}^{t-1}\right\} - \min\left\{F_{id}^t, F_{id}^{t-1}\right\}\right)/f_1\right| \tag{8}$$

$$b_i^t = \frac{1}{n} * \sum_{i=1}^{n}\left(F_i^t - F_{avg}^t\right)/f_2 \tag{9}$$

where u_i^t is the dynamic adjustment coefficient of v_{id}^{t+1}, $t_{\max}$ is the maximum number of iterations. In Eq. (7), ω_0 is the inertia factor in range of [0, 1], k_1 and $k_2 \in$[0, 1]. h_i^t refers to the speed of evolution, b_i^t represents the mean variance of fitness of all particles. In Eqs. (8) and (9), F_{id}^t and F_{id}^{t-1} are the fitness value of pb_{id}^t and pb_{id}^{t-1}, respectively. F_i^t represents the fitness of particle i. F_{avg}^t denotes the average fitness of all particles. f_1 and f_2 are two normalization functions. $f_1 = \max\{\Delta F_1, \Delta F_2, ..., \Delta F_n\}$, $\Delta F_n = \left|F_{id}^t - F_{id}^{t-1}\right|$ and $f_2 = \max\left\{\left|F_1^t - F_{avg}\right|, \left|F_2^t - F_{avg}\right|, ..., \left|F_n^t - F_{avg}\right|\right\}$.

3.4. The Proposed Hybrid GA and IPSO Optimized Cost-Sensitive RBF-NN

3.4.1. Coding scheme

We assume that the maximum number of hidden units in a RBF-NN is N_{max}, and the number of output neurons is S. Each chromosome (or particle) code consists of two parts, as shown in Figure 2. *Part 1* is used to determine the number of hidden units in RBF-NN. In *Part 1*, 1 indicates that the unit is on and 0 is off. The length of *Part 1* is the number of maximum hidden units. As shown in Figure 2, the encoding of *Part 2* is divided into N_{max} segments, and each segment contains the center value ($\boldsymbol{c}_i$), radius value (r_i) of a hidden unit, and the weight ($\boldsymbol{w}$) of hidden units to each output unit. Each segment in *Part 2* corresponds to a code in *Part 1*. In this way, *Part 1* and *Part 2* contain all the information of a hidden layer unit, including its switching state, the center value and the radius value of radial basis function, and its weight to each output unit. *Part 1* and *Part 2* are optimized with GA and IPSO algorithms respectively. They share the same fitness function and evolve into the same direction.

3.4.2. Cost-sensitive fitness function

As to a binary classification problem, the confusion matrix can be represented by Table 1. We use C_{TP} and C_{TN} to represent the costs of TP and TN, respectively. Usually, their values are set as 0. C_{FP} and C_{FN} denote the cost of FP and FN, respectively. In most previous studies, the cost value was often set manually, without considering the impact of sample distribution in the dataset. In this research, the value of C_{FP} is set as imbalance ratio and C_{FN} as 1. In this way, the misclassification cost can be adjusted adaptively according to the sample distribution of different datasets [46,47]. Then, the fitness function can be defined as

$$Fitness = -(IR * C_{FP} + C_{FN}) \tag{10}$$

where IR is imbalance ratio of dataset, $IR = \frac{Majority\ class\ number}{Minority\ class\ number}$.

3.4.3. The main steps of our proposed method

Figure 3 shows the flowchart of the evolutionary self-organizing cost-sensitive RBF-NN optimized by GA and IPSO algorithm (GA-IPSO-CSRBF). The specific process performed by the algorithm is as follows:

1. Data preprocessing, including deleting missing values, removing useless features and standardizing. Divide the original data into training set and testing set.
2. Initialization parameters: population size (PN); maximum number of hidden units (N_{max}); maximum number of iterations (t_{max}); crossover rate and mutation rate of GA (P_c and P_m); individual and social learning factors l_1 and l_2; coefficients k_1 and k_2.
3. Initialize the population based on the initialization parameters.
4. The fitness value of each particle is calculated by Eq. (10). The lower the total cost, the higher the fitness.
5. Apply GA operator (selection, crossover, mutation) to update the structure of RBF-NN. Selection operator uses the roulette wheel selection, which means that the greater the fitness of a particle, the greater the probability that it will be selected. Single-point crossover is used as crossover operator, which indicates selected parents will exchange partly genes at a fixed probability. For the mutation operator, we chose bit-flipping mutation, which changes some genes of a chromosome from 1 to 0 or from 0 to 1.
6. Evolving the center, radius and weight of RBF-NN by Eqs. (3–9).
7. Calculate the fitness of the updated particles. If the best fitness meets the termination condition (best fitness = 0), then output the optimal RBF-NN. Otherwise, return to step 5 until the maximum number of iterations t_{max} is met. Then, output the structure and parameters of RBF-NN corresponding to the particle with the highest fitness.
8. Use optimized cost-sensitive RBF-NN to predict test data.

4. EXPERIMENTS

4.1. Experimental Design

We compare the proposed evolutionary self-organizing cost-sensitive RBF-NN optimized by GA and IPSO (CSRBF) model with three groups of methods. The first group contains the RBF-NN and its two cost-sensitive forms in WEKA [48], including cost-sensitive RBF-NN and meta-cost RBF-NN. These three methods are recorded as

Table 1 | Confusion matrix.

	Actual Positive	Actual Negative
Predicted Positive	True Positive (TP)	False Positive (FP)
Predicted Negative	False Negative (FN)	True Negative (TN)

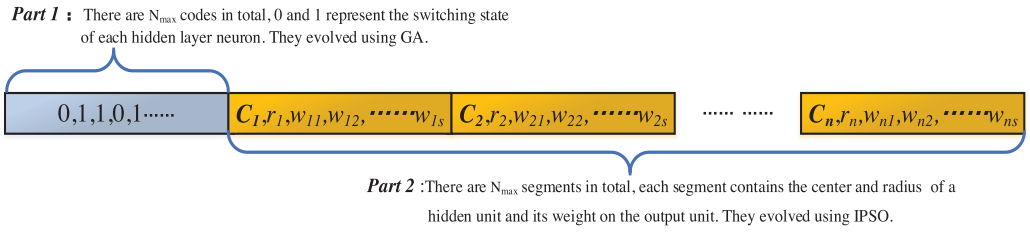

Figure 2 | Coding diagram of a chromosome (or particle).

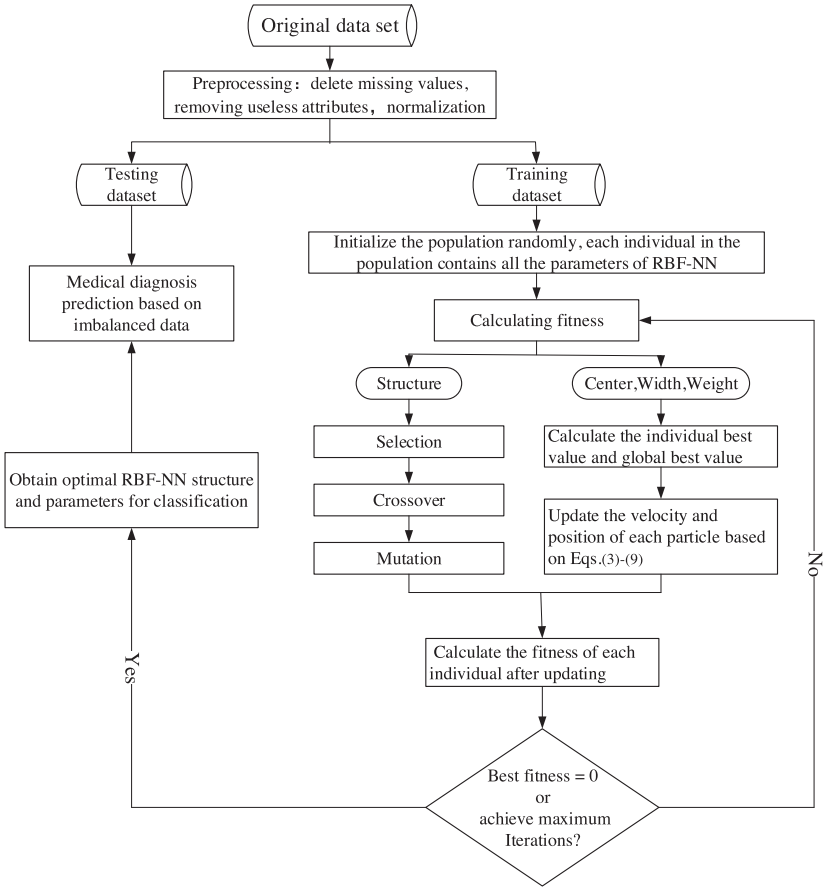

Figure 3 The flowchart of cost-sensitive RBF-NN optimized by GA and IPSO (GA-IPSO-CSRBF) algorithm.

RBF, CS-RBF, and MC-RBF in the experimental results. For the second group, we compare GA-IPSO-CSRBF with ensemble algorithms with RBF-NN as the base classifier, including Adaboost, Logitboost, Bagging, and Voting. The third group consists of three non-cost-sensitive single classifiers including KNN, support vector machine (SVM), and C4.5.

The parameters of GA-IPSO-CSRBF are set as follows: PN = 200, N_{max} = 15, t_{max} = 100, P_c = 0.7, P_m = 0.01, l_1 = l_2 = 2, k_1 = 0.2, and k_2 = 0.4. The proposed algorithm is implemented with Python 3.6, and other comparison algorithms are executed on the WEKA 3.8 platform. All experiments are run on a computer with Intel Core i5 (1.6 GHz, 8 CPUs) and 8 GB RAM. The average performance of these results were reported as the final results in this research.

4.2. Datasets

We selected five imbalanced medical datasets including Wisconsin diagnostic breast cancer dataset (WDBC), Breast cancer Wisconsin (Original) dataset (Breast cancer), Bupa liver disorders dataset (Bupa), Pima Indians diabetes dataset (Pima) from the UCI learning repository, and lower back pain symptoms dataset (LBPS) from Kaggle.com, a large machine learning competition platform. Table 2 shows the details of five datasets.

4.3. Performance Metrics

In this study, accuracy (ACC), true positive rate (TPR), and false positive rate (FPR) are used for evaluating the results. In addition, AUC and the receiver operator characteristic (ROC) curve have been proven to be very suitable in evaluating imbalanced data classification problems [49], so these two indicators are also used in our experimental comparison. The calculation formulas for ACC, TPR, and TFR can be obtained from the confusion matrix in Table 2.

$$ACC = \frac{TN + TP}{TN + TP + FN + FP} \tag{11}$$

$$TPR = \frac{TP}{TP + FN} \tag{12}$$

$$FPR = \frac{FP}{FP + TN} \tag{13}$$

4.4. Experimental Results

4.4.1. Comparison with RBF-NN and its cost-sensitive forms

Table 3 presents a comparison between our GA-IPSO-CSRBF algorithm and RBF, CS-RBF, and MC-RBF in term of ACC on the five

datasets. We can see from Table 3 that the GA-IPSO-CSRBF algorithm can achieve the best performance among the four methods with average results of 95.7% ACC in WDBC dataset, 96.4% in Breast cancer dataset, 68.4% in Bupa dataset, 74.4% in Pima dataset, and 80.9% in LBPS dataset.

AUC results of GA-IPSO-CSRBF, RBF, CS-RBF, and MC-RBF are shown in Table 4. All the AUC values of GA-IPSO-CSRBF are greater than 0.5, indicating that its experimental results are acceptable. The compared results in Table 4 show that the AUC values of our proposed method are 0.990 in WDBC dataset, 0.994 in Breast cancer dataset, 0.724 in Bupa dataset, 0.801 in Pima dataset, and 0.885 in LBPS dataset, which are also better than the other three algorithms.

To further evaluate the robustness of the GA-IPSO-CSRBF algorithm to imbalanced data, we compare it with the other three methods, including RBF, CS-RBF, and MC-RBF in the case of the ROC curves. Figure 4 shows the ROC curves based on the five datasets. As shown in Figure 4, for the Bupa, Pima, and LBPS datasets, we can clearly see that the area under the curve of the GA-IPSO-CSRBF algorithm is larger than the other three methods. For the WDBC and breast cancer datasets, although the area under the curve of the other three methods is already very close to 1, our proposed algorithm still has certain advantages. This indicates that our GA-IPSO-CSRBF performs better than RBF, CS-RBF, and MC-RBF in processing imbalanced data of medical diagnosis.

Table 2 | Details of the selected datasets.

Datasets	Number of Instances	Number of Attributes	Class Distribution
WDBC	569	31	357/212
Breast cancer	699	9	458/241
Bupa	345	6	200/145
Pima	768	8	500/268
LBPS	310	12	210/100

WDBC, Wisconsin diagnostic breast cancer dataset; LBPS, lower back pain symptoms dataset.

Table 3 | GA-IPSO-CSRBF compare RBF, CS-RBF, and MC-RBF in terms of ACC.

Datasets	GA-IPSO-CSRBF	RBF	CS-RBF	MC-RBF
WDBC	0.957	0.947	0.947	0.924
Breast cancer	0.964	0.961	0.961	0.956
Bupa	0.684	0.641	0.583	0.495
Pima	0.744	0.743	0.687	0.691
LBPS	0.809	0.753	0.731	0.699

WDBC, Wisconsin diagnostic breast cancer dataset; LBPS, lower back pain symptoms dataset; GA-IPSO-CSRBF, cost-sensitive RBF-NN optimized by GA and IPSO algorithm; ACC, accuracy.

Table 4 | GA-IPSO-CSRBF compare RBF, CS-RBF, and MC-RBF in terms of AUC.

Datasets	GA-IPSO-CSRBF	RBF	CS-RBF	MC-RBF
WDBC	0.990	0.980	0.979	0.989
Breast cancer	0.994	0.989	0.990	0.976
Bupa	0.724	0.682	0.681	0.511
Pima	0.801	0.754	0.751	0.723
LBPS	0.885	0.839	0.841	0.752

WDBC, Wisconsin diagnostic breast cancer dataset; LBPS, lower back pain symptoms dataset; GA-IPSO-CSRBF, cost-sensitive RBF-NN optimized by GA and IPSO algorithm; AUC, area under curve.

4.4.2. Comparison with different ensemble algorithms

Table 5 shows the comparison between the GA-IPSO-CSRBF algorithm and four ensemble learning methods, including adaboost, logitboost, bagging, and voting in term of ACC on the selected five datasets. Overall, the performance of GA-IPSO-CSRBF is better than several other ensemble algorithms based on RBF-NN. Only for the breast cancer dataset, the accuracy of the GA-IPSO-CSRBF algorithm is slightly lower than logitboost, which is 0.964. But our method outperforms logitboost for the other four datasets. So in general, our proposed method GA-IPSO-CSRBF performs better than logitboost.

Table 6 further compares the performance of GA-IPSO-CSRBF, adaboost, logitboost, bagging, and voting in terms of AUC. As shown in Table 6, the AUC values of our proposed algorithm are larger than other ensemble algorithms for five datasets, except for the bagging for the WDBC dataset. But the performance of bagging is inferior to GA-IPSO-CSRBF for the other four datasets. So overall, our proposed algorithm still has the best performance comparison among the ensemble learning methods.

Figure 5 demonstrates the ROC curves for GA-IPSO-CSRBF compare to adaboost, logitboost, bagging, and voting based on the five datasets. In other words, the proposed GA-IPSO-CSRBF algorithm is more robust than several other ensemble methods, so it can make more reliable decisions on medical diagnostic problems based on imbalanced data.

Table 5 | GA-IPSO-CSRBF compare Adaboost, Logitboost, Bagging, and Voting in terms of ACC.

Datasets	GA-IPSO-CSRBF	Adaboost	Logitboost	Bagging	Voting
WDBC	0.957	0.947	0.918	0.953	0.947
Breast cancer	0.964	0.956	0.966	0.961	0.961
Bupa	0.684	0.680	0.583	0.631	0.641
Pima	0.744	0.735	0.691	0.691	0.743
LBPS	0.809	0.769	0.742	0.763	0.753

WDBC, Wisconsin diagnostic breast cancer dataset; LBPS, lower back pain symptoms dataset; GA-IPSO-CSRBF, cost-sensitive RBF-NN optimized by GA and IPSO algorithm; ACC, accuracy.

Table 6 | GA-IPSO-CSRBF compare Adaboost, Logitboost, Bagging, and Voting in terms of AUC.

Datasets	GA-IPSO-CSRBF	Adaboost	Logitboost	Bagging	Voting
WDBC	0.990	0.989	0.969	0.993	0.980
Breast cancer	0.994	0.988	0.991	0.991	0.989
Bupa	0.724	0.641	0.438	0.630	0.682
Pima	0.801	0.746	0.653	0.735	0.754
LBPS	0.885	0.849	0.759	0.843	0.839

WDBC, Wisconsin diagnostic breast cancer dataset; LBPS, lower back pain symptoms dataset; GA-IPSO-CSRBF, cost-sensitive RBF-NN optimized by GA and IPSO algorithm; AUC, area under curve.

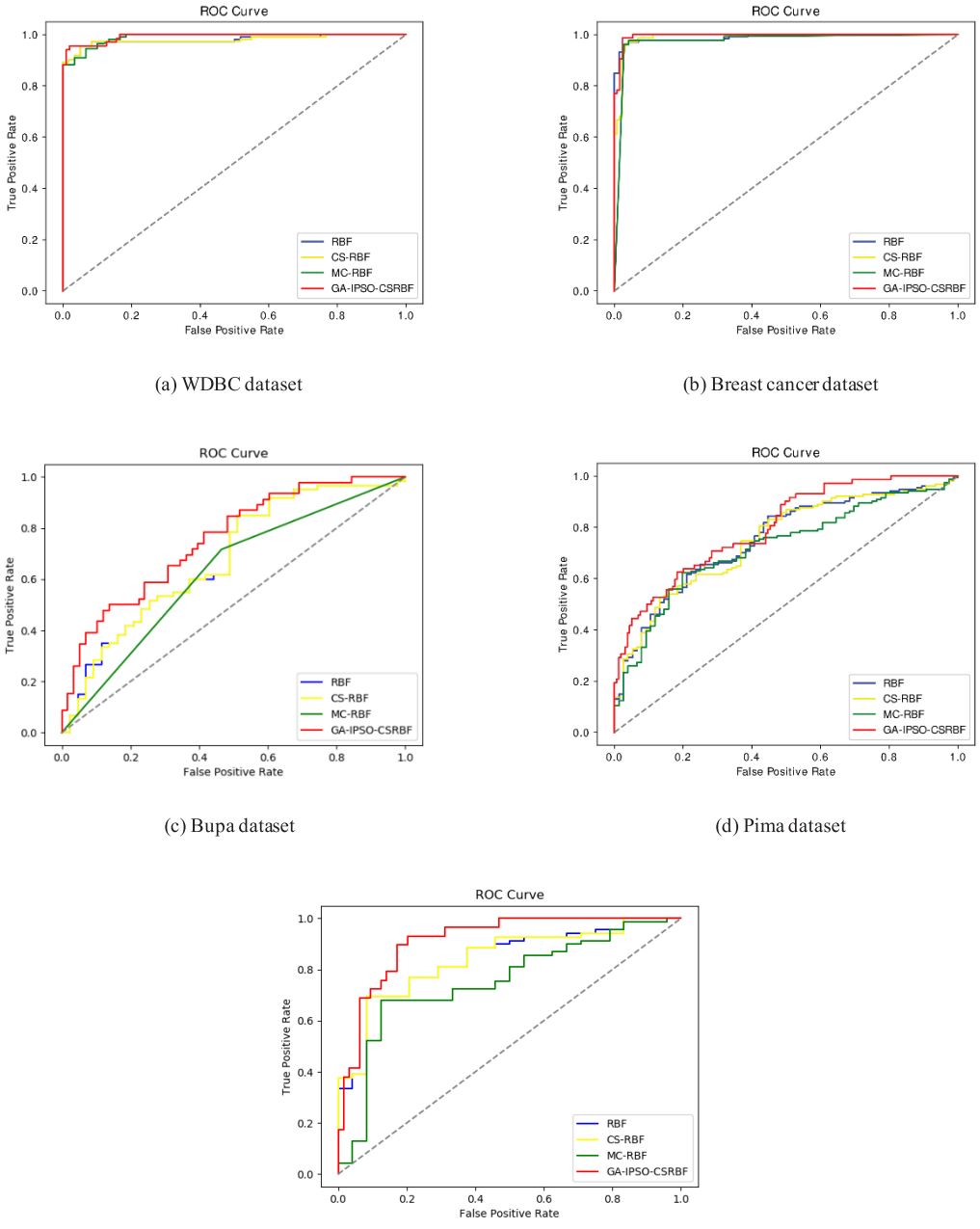

(a) WDBC dataset

(b) Breast cancer dataset

(c) Bupa dataset

(d) Pima dataset

(e) LBPS dataset

Figure 4 The receiver operator characteristic (ROC) curves for cost-sensitive RBF-NN optimized by GA and IPSO (GA-IPSO-CSRBF) compared to RBF, CS-RBF, and MC-RBF based on the five datasets.

4.4.3. Comparison with different non-cost-sensitive single classifiers

Table 7 presents a comparison of our GA-IPSO-CSRBF algorithm with KNN, SVM, and C4.5 in term of ACC on the five datasets. We can see from Table 7 that the proposed GA-IPSO-CSRBF outperforms the other three algorithms as a whole. Closer inspection of the Table 7 shows compared with KNN method, the GA-IPSO-CSRBF method achieves a slightly inferior performance on breast cancer dataset with average results of 96.4% ACC. But its performance is significantly better than KNN on other four datasets. This shows that the GA-IPSO-CSRBF method is generally better than KNN.

AUC performance results of GA-IPSO-CSRBF, KNN, SVM, and C4.5 are shown in Table 8. From these compared results, we can see that our GA-IPSO-CSRBF classifier achieves the best performance among all of the algorithms used to compare. On the contrary, due to the imbalance of the data distribution, the AUC value of SVM is only 0.5 for the WDBC and Pima datasets, which is the lowest in the compared classifier.

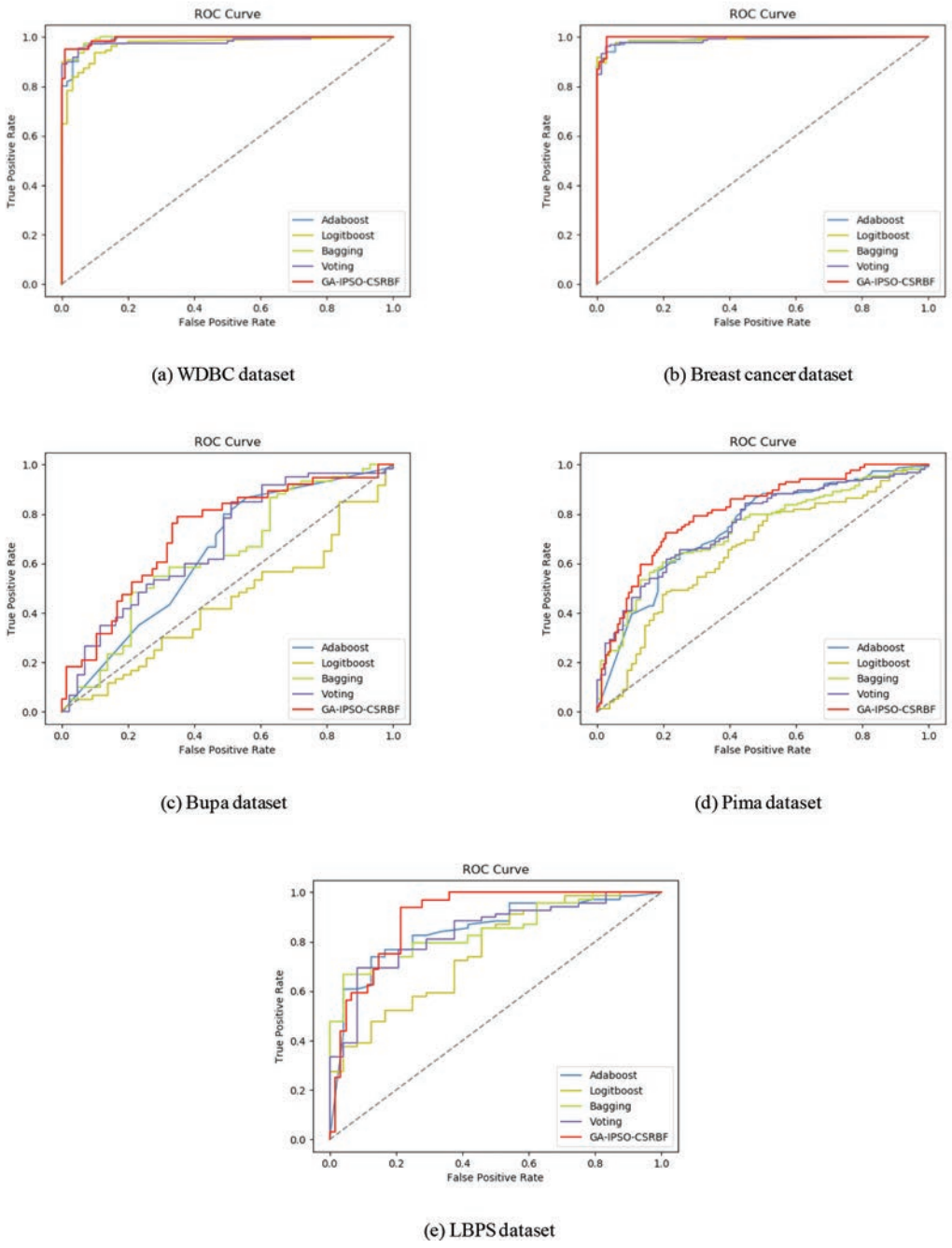

Figure 5 | The receiver operator characteristic (ROC) curves for cost-sensitive RBF-NN optimized by GA and IPSO (GA-IPSO-CSRBF) compare to Adaboost, Logitboost, Bagging, and Voting based on the five datasets.

Table 7 | GA-IPSO-CSRBF compare KNN, SVM, and C4.5 in terms of ACC.

Datasets	GA-IPSO-CSRBF	KNN	SVM	C4.5
WDBC	0.957	0.953	0.649	0.947
Breast cancer	0.964	0.966	0.941	0.902
Bupa	0.684	0.641	0.592	0.667
Pima	0.744	0.722	0.669	0.726
LBPS	0.809	0.634	0.742	0.796

WDBC, Wisconsin diagnostic breast cancer dataset; LBPS, lower back pain symptoms dataset; GA-IPSO-CSRBF, cost-sensitive RBF-NN optimized by GA and IPSO algorithm; KNN, k-nearest neighbor; SVM, support vector machine; ACC, accuracy.

Table 8 | GA-IPSO-CSRBF compare KNN, SVM, and C4.5 in terms of AUC.

Datasets	GA-IPSO-CSRBF	KNN	SVM	C4.5
WDBC	0.990	0.949	0.500	0.949
Breast cancer	0.994	0.981	0.952	0.931
Bupa	0.724	0.626	0.512	0.638
Pima	0.801	0.676	0.500	0.673
LBPS	0.885	0.591	0.500	0.601

WDBC, Wisconsin diagnostic breast cancer dataset; LBPS, lower back pain symptoms dataset; GA-IPSO-CSRBF, cost-sensitive RBF-NN optimized by GA and IPSO algorithm; KNN, k-nearest neighbor; SVM, support vector machine; AUC, area under curve.

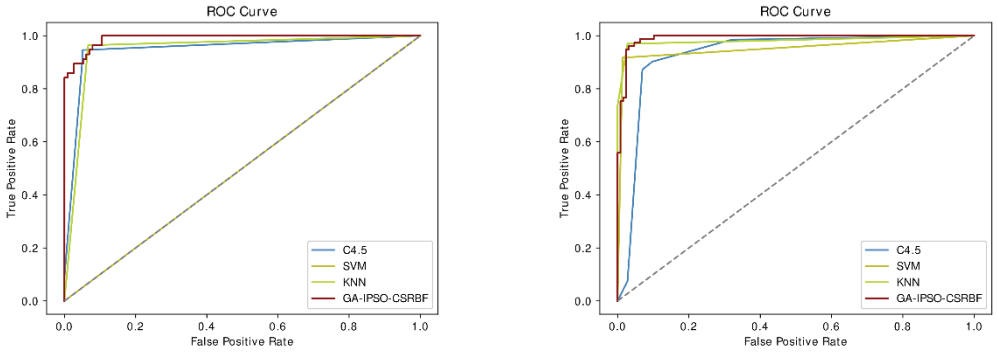

(a) WDBC dataset

(b) Breast cancer dataset

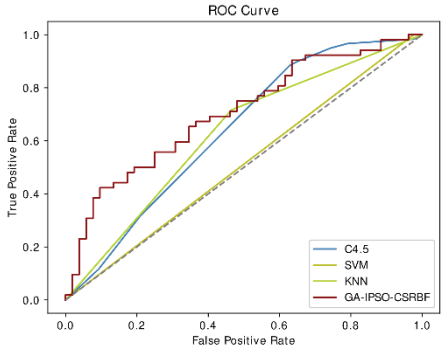

(c) Bupa dataset

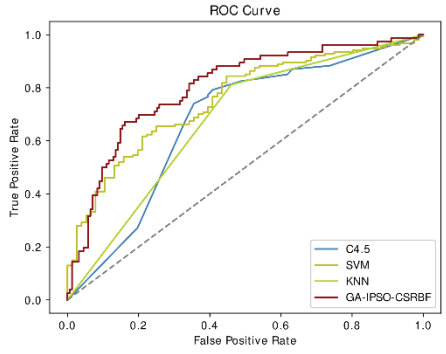

(d) Pima dataset

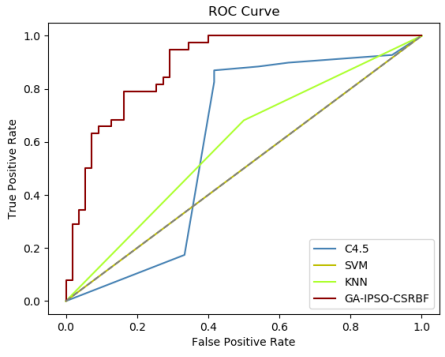

(e) LBPS dataset

Figure 6 The receiver operator characteristic (ROC) curves for cost-sensitive RBF-NN optimized by GA and IPSO (GA-IPSO-CSRBF) compared to C4.5, support vector machine (SVM), and k-nearest neighbor (KNN) based on the five datasets.

To further evaluate the robustness of our method to imbalanced data, we compare it with the other three common methods, including KNN, SVM, and C4.5 regard to the ROC curves. Figure 6 shows the ROC curves based on the five datasets. As shown in Figure 6, the proposed GA-IPSO-CSRBF classifier has demonstrated obvious advantages compared to other three common classifiers. This means that our GA-IPSO-CSRBF performs better than KNN, SVM, and C4.5 in processing imbalanced data of medical diagnosis.

4.5. Discussion

From the above experimental results, it can be seen that our GA-IPSO-CSRBF algorithm not only has a higher accuracy, but also has a larger AUC value than other comparison methods for five different imbalanced medical datasets. This shows that the proposed algorithm can improve the recognition of minority class while taking into account the overall classification accuracy. The reasons are as follows: firstly, we set a larger misclassification cost for the

minority class, which makes the proposed algorithm pay more attention to the minority class. Moreover, the objective function of GA-IPSO-CSRBF is to minimize the total misclassification cost, which ensures the overall performance. Thirdly, the misclassification cost of the minority class is set to the imbalanced rate so that the proposed algorithm can adapt to datasets with different sample distributions.

For medical data, the cost of misclassification of minority samples (positive samples) is often higher. The cost of misclassifying a patient as a healthy person is far greater than the cost of misclassifying a healthy person as a patient. GA-IPSO-CSRBF can give more attention to the minority samples and at the same time obtain a good overall performance, so it is more suitable for imbalanced medical data than other comparison algorithms.

5. CONCLUSIONS

In this research, we propose an evolutionary self-organizing cost-sensitive RBF-NN which are jointly optimized by GA and IPSO to handle medical imbalanced data. This method can adaptively optimize both the structure and parameters of cost-sensitive RBF-NN simultaneously. The effectiveness of our proposed approach is tested on five imbalanced medical diagnosis datasets. The experimental results indicate that the proposed model is superior to other comparison methods in terms of accuracy and AUC.

For different medical diagnosis datasets, the proposed model can adaptively generate appropriate structure and parameters of RBF-NN. The cost-sensitive fitness function allows it can more focus on the minority class samples with higher cost of misclassification while taking into account the overall classification accuracy, so it can effectively improve the accuracy of medical diagnosis and reduce the error rate of medical decisions. Moreover, our proposed algorithm has a higher AUC value than other methods, indicating that it has better robustness for processing imbalanced data for medical diagnosis, which is crucial for both doctors and patients.

Although our research has made some progress, there is still much room for improvement in the future. Future research can try to use other representative computational intelligence methods to solve this problem, such as monarch butterfly optimization (MBO) [50], earthworm optimization algorithm (EWA) [51], elephant herding optimization (EHO) [52], and moth search (MS) algorithm [53].

CONFLICTS OF INTEREST

The authors declare no conflicts of interest.

AUTHORS' CONTRIBUTIONS

All authors contributed to the work, and all authors read and approved the final manuscript.

Funding Statement

This research is supported by the National Natural Science Foundation of China (Grant No.: 71571105).

ACKNOWLEDGMENTS

We sincerely thank all reviewers and editors for their careful work and considerations on this paper.

REFERENCES

[1] J.S.M. Alneamy, *et al.*, Utilizing hybrid functional fuzzy wavelet neural networks with a teaching learning-based optimization algorithm for medical disease diagnosis, Comput. Biol. Med. 112 (2019), 103348.
[2] S. Shilaskar, A. Ghatol, P. Chatur, Medical decision support system for extremely imbalanced datasets, Inf. Sci. 384 (2017), 205–219.
[3] X. Tao, *et al.*, Affinity and class probability-based fuzzy support vector machine for imbalanced data sets, Neural Netw. 122 (2020), 289–307.
[4] D. Gan, *et al.*, Integrating TANBN with cost sensitive classification algorithm for imbalanced data in medical diagnosis, Comput. Ind. Eng. 140 (2020), 106266.
[5] S. García, *et al.*, Dynamic ensemble selection for multi-class imbalanced datasets, Inf. Sci. 445 (2018), 22–37.
[6] S. Pouyanfar, S.-C. Chen, Automatic video event detection for imbalance data using enhanced ensemble deep learning, Int. J. Semant. Comput. 11 (2017), 85–109.
[7] R.J. Kuo, *et al.*, Integrating cluster analysis with granular computing for imbalanced data classification problem - a case study on prostate cancer prognosis, Comput. Ind. Eng. 125 (2018), 319–332.
[8] Z.-L. Zhang, *et al.*, Cost-Sensitive back-propagation neural networks with binarization techniques in addressing multi-class problems and non-competent classifiers, Appl. Soft Comput. 56 (2017), 357–367.
[9] P. Domingos, MetaCost: a general method for making classifiers cost-sensitive, in Conference on Knowledge Discovery and Data Mining, San Diego, CA, USA, 1999.
[10] C.-h. Tsai, L.-c. Chang, H.-c. Chiang, Forecasting of ozone episode days by cost-sensitive neural network methods, Sci. Total Environ. 407 (2009), 2124–2135.
[11] S. Zhang, Cost-sensitive KNN classification, Neurocomput. 391 (2020), 234–242.
[12] A. Ghodsi, D. Schuurmans, Automatic basis selection techniques for RBF networks, Neural Netw. 16 (2003), 809–816.
[13] S. Yu, K. Wang, Y.-M. Wei, A hybrid self-adaptive particle swarm optimization–genetic algorithm–radial basis function model for annual electricity demand prediction, Energy Convers. Manag. 91 (2015), 176–185.
[14] V. Fathi, G.A. Montazer, An improvement in RBF learning algorithm based on PSO for real time applications, Neurocomput. 111 (2013), 169–176.
[15] S. Amini, M. Taki, A. Rohani, Applied improved RBF neural network model for predicting the broiler output energies, Appl. Soft Comput. 87 (2020), 106006.
[16] P. Kumudha, R. Venkatesan, Cost-sensitive radial basis function neural network classifier for software defect prediction, Sci. World J. 2016 (2016), 1–20.
[17] R. Mohammadi, S.M.T. Fatemi Ghomi, F. Zeinali, A new hybrid evolutionary based RBF networks method for forecasting time

series: a case study of forecasting emergency supply demand time series, Eng. Appl. Artif. Intell. 36 (2014), 204–214.
[18] Z.-Q. Li, *et al.*, A proposed self-organizing radial basis function network for aero-engine thrust estimation, Aerospace Sci. Technol. 87 (2019), 167–177.
[19] W. Jia, D. Zhao, L. Ding, An optimized RBF neural network algorithm based on partial least squares and genetic algorithm for classification of small sample, Appl. Soft Comput. 48 (2016), 373–384.
[20] G.A. Montazer, D. Giveki, An improved radial basis function neural network for object image retrieval, Neurocomputing. 168 (2015), 221–233.
[21] S. Yu, Y.-M. Wei, K. Wang, Provincial allocation of carbon emission reduction targets in China: an approach based on improved fuzzy cluster and Shapley value decomposition, Energy Policy. 66 (2014), 630–644.
[22] C.-F. Tsai, *et al.*, Under-sampling class imbalanced datasets by combining clustering analysis and instance selection, Inf. Sci. 477 (2019), 47–54.
[23] N. Ofek, *et al.*, Fast-CBUS: a fast clustering-based undersampling method for addressing the class imbalance problem, Neurocomputing. 243 (2017), 88–102.
[24] W.-C. Lin, *et al.*, Clustering-based undersampling in class-imbalanced data, Inf. Sci. 409 (2017), 17–26.
[25] B. Krawczyk, *et al.*, Evolutionary undersampling boosting for imbalanced classification of breast cancer malignancy, Appl. Soft Comput. 38 (2016), 714–726.
[26] M. Galar, *et al.*, EUSBoost: enhancing ensembles for highly imbalanced data-sets by evolutionary undersampling, Pattern Recognit. 46 (2013), 3460–3471.
[27] S. Cateni, V. Colla, M. Vannucci, A method for resampling imbalanced datasets in binary classification tasks for real-world problems, Neurocomputing. 135 (2014), 32–41.
[28] N.V. Chawla, *et al.*, SMOTE: synthetic minority over-sampling technique, J. Artif. Intell. Res. 16 (2002), 321–357.
[29] J.A. Sáez, *et al.*, SMOTE–IPF: addressing the noisy and borderline examples problem in imbalanced classification by a re-sampling method with filtering, Inf. Sci. 291 (2015), 184–203.
[30] G. Douzas, F. Bacao, F. Last, Improving imbalanced learning through a heuristic oversampling method based on k-means and SMOTE, Inf. Sci. 465 (2018), 1–20.
[31] G. Douzas, F. Bacao, Geometric SMOTE a geometrically enhanced drop-in replacement for SMOTE, Inf. Sci. 501 (2019), 118–135.
[32] X.W. Liang, *et al.*, LR-SMOTE — an improved unbalanced data set oversampling based on K-means and SVM, Knowl. Based Syst. 196 (2020), 105845.
[33] G.E. Batista, R.C. Prati, M.C. Monard, A study of the behavior of several methods for balancing machine learning training data, ACM SIGKDD Explor. Newsl. 6 (2004), 20–29.
[34] V. López, *et al.*, An insight into classification with imbalanced data: empirical results and current trends on using data intrinsic characteristics, Inf. Sci. 250 (2013), 113–141.
[35] G. Haixiang, *et al.*, Learning from class-imbalanced data: review of methods and applications, Expert Syst. Appl. 73 (2017), 220–239.
[36] Y. Freund, R.E. Schapire, Experiments with a new boosting algorithm, in International Conference on Machine Learning, Citeseer, Bari, Italy. 1996, p. 148–156.
[37] J.H. Friedman, Greedy function approximation: a gradient boosting machine, Ann. Stat. 29 (2001), 1189–1232.
[38] J. Lin, *et al.*, Accurate prediction of potential druggable proteins based on genetic algorithm and Bagging-SVM ensemble classifier, Artif. Intell. Med. 98 (2019), 35–47.
[39] M. Hao, Y. Wang, S.H. Bryant, An efficient algorithm coupled with synthetic minority over-sampling technique to classify imbalanced PubChem BioAssay data, Anal. Chim. Acta. 806 (2014), 117–127.
[40] V. Bolón-Canedo, A. Alonso-Betanzos, Ensembles for feature selection: a review and future trends, Inf. Fusion. 52 (2019), 1–12.
[41] D. Fuqua, T. Razzaghi, A cost-sensitive convolution neural network learning for control chart pattern recognition, Expert Syst. Appl. 150 (2020), 113275.
[42] H. Li, *et al.*, Cost-sensitive sequential three-way decision modeling using a deep neural network, Int. J. Approx. Reason. 85 (2017), 68–78.
[43] Ö.F. Arar, K. Ayan, Software defect prediction using cost-sensitive neural network, Appl. Soft Comput. 33 (2015), 263–277.
[44] J. Park, I.W. Sandberg, Universal approximation using radial-basis-function networks, Neural Comput. 3 (1991), 246–257.
[45] J.H. Holland, Genetic algorithms, Sci. Am. 267 (1992), 66–73.
[46] V. López, *et al.*, Cost-sensitive linguistic fuzzy rule based classification systems under the MapReduce framework for imbalanced big data, Fuzzy Sets Syst. 258 (2015), 5–38.
[47] C.L. Castro, A.P. Braga, Novel cost-sensitive approach to improve the multilayer perceptron performance on imbalanced data, IEEE Trans. Neural Netw. Learn. Syst. 24 (2013), 888–899.
[48] M. Hall, *et al.*, The WEKA data mining software: an update, SIGKDD Explor. Newsl. 11 (2009), 10–18.
[49] D. Veganzones, E. Severin, An investigation of bankruptcy prediction in imbalanced datasets, Decis. Support Syst. 112 (2018), 111–124.
[50] Y. Feng, *et al.*, Multi-strategy monarch butterfly optimization algorithm for discounted {0-1} knapsack problem, Neural Comput. Appl. 30 (2017), 3019–3036.
[51] G.G. Wang, S. Deb, L.D.S. Coelho, Earthworm optimisation algorithm: a bio-inspired metaheuristic algorithm for global optimisation problems, Int. J. Bio-Inspired Comput. 12 (2015), 1–22.
[52] G.G. Wang, *et al.*, A new metaheuristic optimisation algorithm motivated by elephant herding behaviour, Int. J. Bio Inspired Comput. 8 (2017), 394–409.
[53] G.G. Wang, Moth search algorithm: a bio-inspired metaheuristic algorithm for global optimization problems, Memet. Comput. 10 (2016), 151–164.